Towards the β function of $\mathrm{SU}(2)$ with adjoint matter using Pauli–Villars fields

Ed Bennett,^{a,*} **Andreas Athenodorou,**^{b} **Georg Bergner,**^{c} **Pietro Butti**^{d,e} **and Biagio Lucini**^{a,f}

^{a}*Swansea Academy of Advanced Computing, Swansea University, Bay Campus, Fabian Way, Swansea SA1 8EN, United Kingdom*

^{b}*Computation-based Science and Technology Research Center, The Cyprus Institute, 20 Kavafi Str., Nicosia 2121, Cyprus*

^{c}*University of Jena, Institute for Theoretical Physics, Max-Wien-Platz 1, D-07743 Jena, Germany*

^{d}*Departamento de Física Teórica, Facultad de Ciencias and Centro de Astropartículas y Física de Altas Energías (CAPA), Universidad de Zaragoza, Calle Pedro Cerbuna 12, E-50009, Zaragoza, Spain*

^{e}*Quantum Field Theory Center (ℏQTC) at IMADA & D-IAS, Southern Denmark University, Campusvej 55, 5230 Odense M, Denmark*

^{f}*Department of Mathematics, Swansea University, Fabian Way, Swansea SA1 8EN, UK*
  E-mail: e.j.bennett@swansea.ac.uk, a.athenodorou@cyi.ac.cy, georg.bergner@uni-jena.de, pbutti@qtc.sdu.dk, b.lucini@swansea.ac.uk

The family of SU(2) theories with matter transforming in the adjoint representation has attracted interest from many angles. The two-flavour theory, known as Minimal Walking Technicolor, has a body of evidence pointing to it being in the conformal window with anomalous dimension $\gamma_* \approx 0.3$. Perturbative calculations would suggest that the one-flavour theory should be confining and chirally broken; however, lattice studies of the theory have been inconclusive. In this contribution we present a first look at efforts towards the computation of the beta function of these theories using the gradient flow methodology. Following an exploration of the phase diagram of the two theories with Wilson fermions and additional Pauli–Villars fields, we tune the bare fermion mass to near the chiral limit, and subsequently generate ensembles at five lattice volumes and a range of lattice spacings.

---

*Speaker

1. Introduction

In the last two decades the SU(2) gauge theories with various numbers N_f of adjoint fermion flavours have been studied extensively on the lattice. This family of theories is interesting in a number of contexts: the $N_f = 2$ theory, for example, provides the minimal possible realisation of Walking Technicolor. Numerous studies have placed it in the conformal window; recent work [1] shows a mass anomalous dimension of 0.304(4) at finite lattice spacing from the scaling of the Dirac mode number, while earlier step-scaling studies [2] indicate an anomalous dimension of $0.263(4)^{+0.012}_{-0.015}$. The $N_f = 1$ theory cannot by itself break electroweak symmetry, although it can be extended in such a direction in theories such as Ultra Minimal Walking Technicolor, and is interesting in the context of being able to identify the lower end of the conformal window, and to observe near-conformal behaviour. It is also relevant to studies of topological phase transitions via 't Hooft anomaly matching. Recent work [1] finds a relatively small continuum limit mass anomalous dimension of 0.170(7) by extrapolating values computed using the mode number at finite lattice spacing.

The fixed point in the $N_f = 2$ theory, and any possible remnant of a fixed point in the $N_f = 1$ theory, can only be found at relatively strong coupling. Such couplings are challenging to reach on the lattice, as in this regime the lattice spacing becomes large, and a bulk phase transition can mean that results are not connected to the continuum limit. Recent work [3, 4] has suggested that introducing Pauli–Villars (PV) fields into the action may reduce lattice artefacts at strong coupling and hence widen the range of couplings at which a theory may be studied.

2. Summary of the theory

We generate ensembles using the Wilson gauge action $S_G = \beta_0 \sum_p \text{Tr} \left[1 - \frac{1}{2} U(p) \right]$ and Wilson fermion action, $S_F = \sum_{\alpha=1}^{N_f} \overline{\psi}_\alpha(x)(i\slashed{D} - m)\psi_\alpha(x)$, where $N_f \in \{1, 2\}$, as in our previous work [1]. To this, we add N_{PV} species of PV field each with mass m_{PV}, implemented as a Hasenbusch mass term with a very heavy mass in the denominator.

While previous work [3, 4] has smeared these PV fields, in this work we use unsmeared fields. Theoretically, since this has the effect of adding a single plaquette contribution to the action, this would be expected to have no effect on the lattice artefacts, leading mainly to a shift in the value of β_0. In this work we will test that prediction.

We make use of the RHMC and HMC algorithms respectively for $N_f = 1$ and 2. The HiRep [5–7] code is used in both cases, and is run both on CPU (for the phase diagram) and on A100 GPUs (for larger volumes). GNU Parallel [8] is used to manage large swarms of small jobs. Meson correlation function and gradient flow histories are computed using HiRep on CPUs.

3. Parameter tuning

Since we expect the PV fields to affect the region of parameter space accessible to computation, we must map out that parameter space to identify the region to study. We study the average plaquette on an 8^4 lattice as a function of β_0 and m_f, for both $N_f = 1$ and 2, with $N_{PV} = 5$, 10, and 15, each with $m_{PV} = 0.5$ and 1.0. We also include the case $N_{PV} = 0$ for comparison. We show the resulting phase diagrams in Fig. 1; the shift in β_0 is clearly visible here. Based on this, we identify regions of β_0 to target for $N_f = 1$, $N_{PV} \in \{5, 10, 15\}$, $m_{PV} = 0.5$ and $N_f = 2$, $N_{PV} = 15$, $m_{PV} = 0.5$.
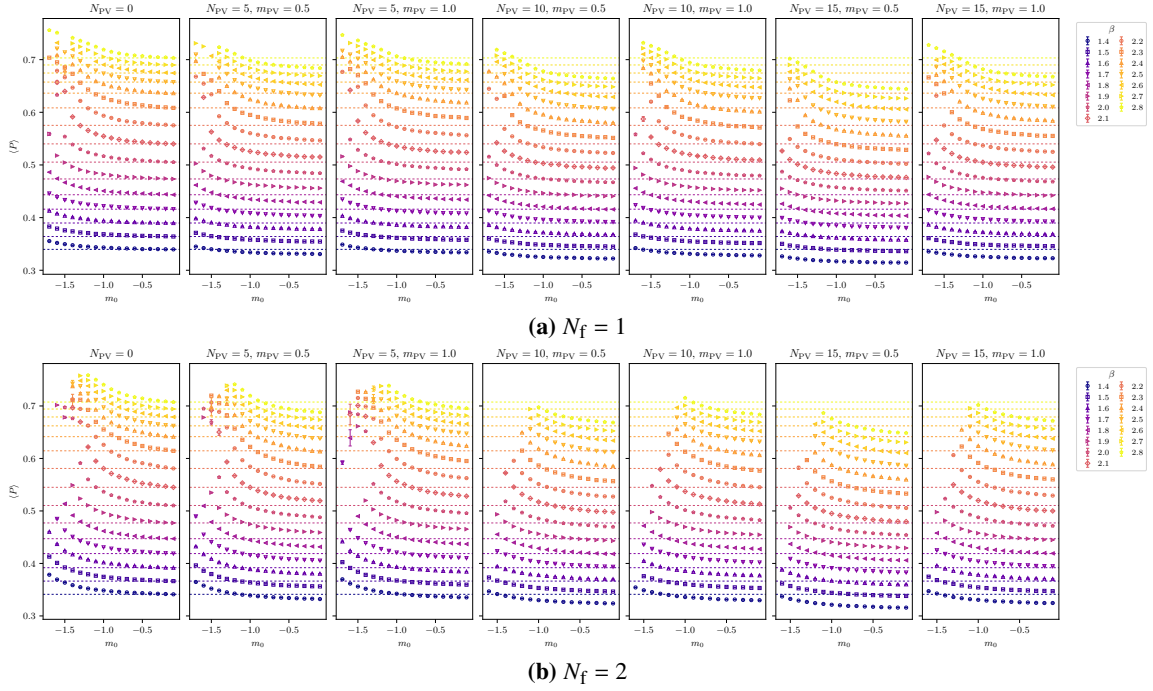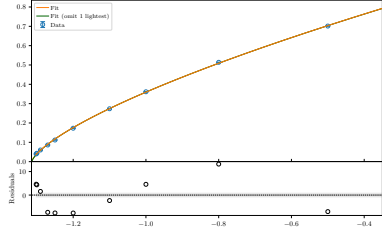
(a) $N_f = 1$

(b) $N_f = 2$

Figure 1: Phase diagram of the theory with (a) $N_f = 1$ and (b) $N_f = 2$ flavours of Dirac fermion in the adjoint representation, with $N_{PV} \in \{0, 5, 10, 15\}$ and $m_{PV} \in \{0.5, 1.0\}$ (panels left to right). The average plaquette is plotted as a function of the bare fermion mass $m_f \in [-1.7, -0.1]$ (horizontal axis) and the bare coupling $\beta_0 \in [1.8, 2.8]$ (colours). For each value of β_0, the value of the heaviest mass $m = -0.1$ is projected across all panels as dashed lines of the same colour, to allow easier comparison.

(a) $N_f = 1$, $N_{PV} = 15$, $m_{PV} = 0.5$, $\beta = 2.7$
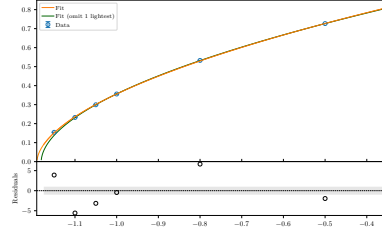
(b) $N_f = 2$, $N_{PV} = 5$, $m_{PV} = 0.5$, $\beta = 2.35$

Figure 2: The PCAC fermion mass as a function of the bare fermion mass for two specific choices of N_f, N_{PV}, mPV, β. In addition to the data, the fit line and residual at each point are also shown.

To compute the β function, we aim to simulate at or very close to the chiral limit. Because the Wilson fermion action introduces an additive renormalisation to the fermion mass, it is necessary to tune the bare fermion mass m_0 to find the chiral limit for each value of N_{PV}, m_{PV}, β_0 considered. To do this, in each case, a range of ensembles are generated on a 32×16^3 volume, and the PCAC mass [9] is computed. This is then extrapolated to the chiral limit using $m_{PCAC} = B(m_0 - m_0^{cr})^C$, where B, C, and m_0^{cr} are fit parameters, the latter of which is the chiral limit bare mass that is used for full ensemble generation. Examples of this extrapolation are shown in Fig. 2.

3

4. Computing the running coupling and β function

In this section we will summarise the methodology of computing the running coupling and β function described by the authors of Ref. [4], to which we refer for further detail.

We may evolve our field configurations under the diffusion equation defined by the gradient of the Wilson action (the Wilson flow), as described in Ref. [10]. The running coupling at finite volume and lattice spacing can be computed as a function of the flow time t as $g_{\mathrm{GF}}^2(t; L, g_0^2) = \langle t^2 E(t) \rangle$, where the energy density E may be computed on the lattice via a variety of operators; in this work we consider the plaquette and clover operators. From this, the β function may be computed as $\beta(t; L, g_{0^2}) = t \frac{\mathrm{d}}{\mathrm{d}t} g_{\mathrm{GF}}^2(t; L, g_0^2)$, where we may fit subsets of the volumes considered, and compute the fit results' mean weighted using a modified Akaike Information Criteria.

Both g_{GF}^2 and β may be extrapolated to the infinite-volume limit using a linear fit form in the reciprocal of the lattice volume

$$g_{\mathrm{GF}}^2(t; L, g_0^2) = g_{\mathrm{GF}}^2(t; g_0^2) + C_{g^2} L^{-4} , \qquad \beta(t; L, g_0^2) = \beta(t; g_0^2) + C_\beta L^{-4} . \qquad (1)$$

These may then be interpolated against each other to obtain the β function at arbitrary g_{GF}^2, using

$$\beta^{\mathrm{int}}(t, g_{\mathrm{GF}}^2) = g_{\mathrm{GF}}^4 \sum_{n=0}^{N-1} p_n g_{\mathrm{GF}}^{2n} , \qquad (2)$$

where N is fixed to the lowest value that gives a reasonable fit. This allows the β function to be scanned across a range of running couplings, and at each of these a continuum limit may be taken by extrapolating the linear Ansatz

$$\beta^{\mathrm{int}}(t, g_{\mathrm{GF}}^2) = \beta^{\mathrm{cont}}(g_{\mathrm{GF}}^2) + \frac{C_{\mathrm{cont}}}{t} . \qquad (3)$$

5. Analysis workflow

The data analysis pipeline is written using Snakemake [11], connecting individual tools each of which makes use of pyerrors [12]. This allows simple rules (for example, how to transform one or more input data files to an output containing one or more statistical quantities) to be easily composed, independent steps to be parallelised, and redundant computations to be skipped. To generate every plot in this contribution, excluding Fig. 4, starting from the raw output files transferred from the HPC resources used to generate them, requires the single command:

```
snakemake --cores 6 --use-conda
```

be run twice, once per N_{f}. This then launches 344 (for $N_{\mathrm{f}} = 1$) + 81 (for $N_{\mathrm{f}} = 2$) job steps, taking 5 minutes to run on six cores of an Apple M1 Pro CPU. All required software packages are installed automatically; no setup is required beyond installing Snakemake.

An illustration of the workflow is shown in Fig. 3; each rule (orange hexagon) may be run many times with different inputs to produce different output files. If only one input file has changed since the previous execution, then only the steps that directly or indirectly depend on that input are re-run.

In order to verify that the implementation of the analysis was correct, a modified version of the workflow was applied to the open dataset [13] used to prepare Ref. [4]. The workflow reproduces
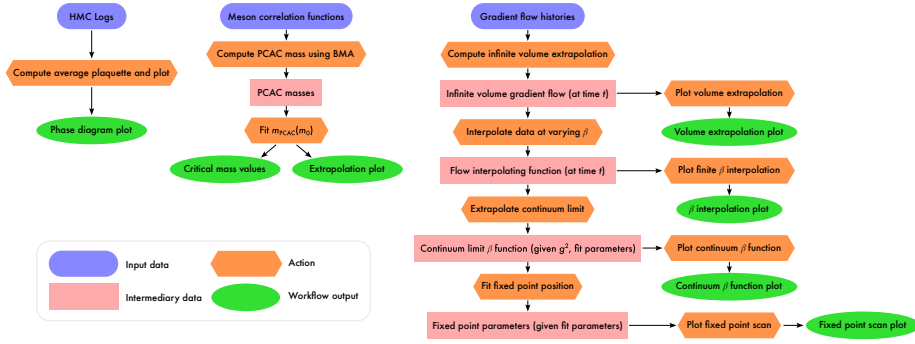
Figure 3: Diagram of the analysis workflow used. Blue lozenges represent input data, generated using HPC facilities and copied off for analysis. Pink rectangles represent intermediary data files, which are automatically generated and updated as necessary by the workflow. Orange hexagons represent specific rules, transforming input to output files. Green ellipses represent output files, either data or plots. Each may have multiple instances, for different input parameters. (For example, there is more than one extrapolation plot of m_{PCAC} produced, each relies on more than one m_{PCAC} value, each requiring an execution of the effective mass fit.)
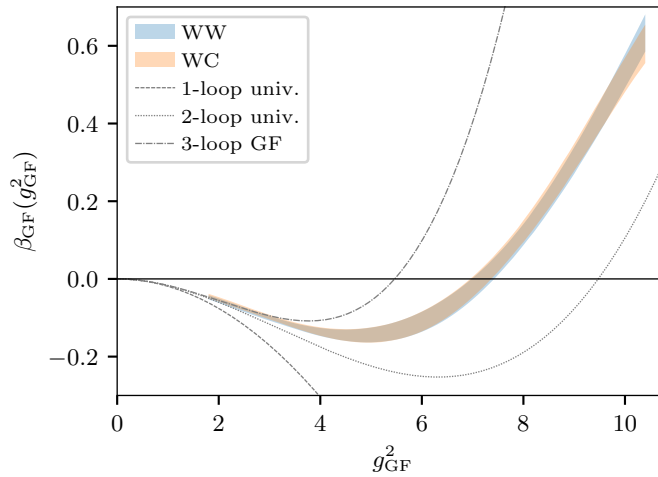
Figure 4: The continuum β function for the SU(3) theory with $N_{\mathrm{f}} = 12$ fundamental flavours, computed using the dataset at Ref. [13]. This qualitatively agrees with Fig. 1 of Ref. [4], which presented the first analysis of the same data.

the finding of a conformal fixed point in the β function of the SU(3) theory with 12 fundamental Dirac flavours. Reproducing every figure[1] of Ref. [4] from the released data requires the same single command as above, which launches 4,227 job steps, and takes 19 minutes on six cores of an Apple M1 Pro CPU. The results, such as the continuum β-function shown in Fig. 4 are qualitatively consistent; small differences in the numerical results (for example, finding the fixed point at $g_{\mathrm{GF}}^2 \approx 7.0$ rather than 6.5) are likely due to subtly different weights in some extrapolations.

---

[1]Excluding Fig. 2, the data for which were not released, and Fig. 9, which is not directly relevant to this work.
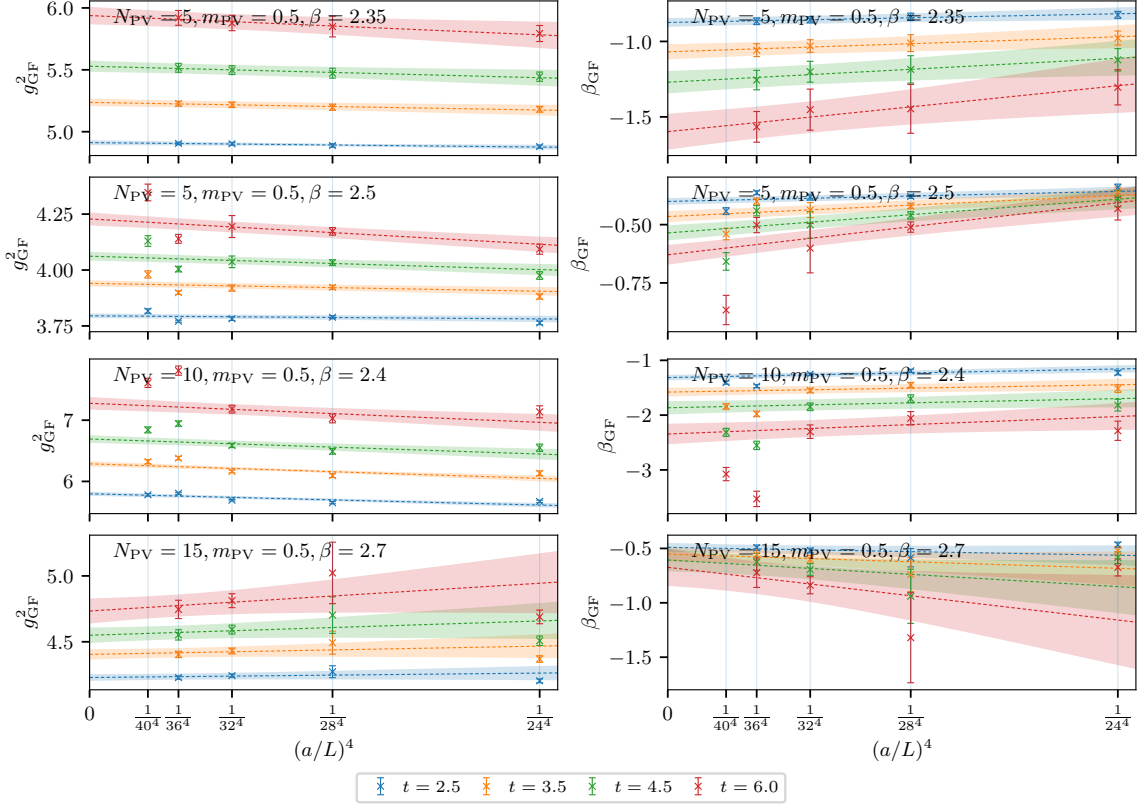
Figure 5: The finite-volume data (points) and infinite volume extrapolations using Eq. (1) (bands) of the running coupling (left) and the β function (right) of the theory with $N_f = 2$ at four values of the flow time $t \in \{2.5, 3.5, 4.5, 6.0\}$, for the four cases $(N_{PV} = 5, \beta = 2.35)$, $(N_{PV} = 5, \beta = 2.5)$, $(N_{PV} = 10, \beta = 2.4)$, and $N_{PV} = 15, \beta = 2.7$. $m_{PV} = 0.5$ in all cases. Blue vertical lines indicate the volumes studied in this work; where points are missing, the relevant data have not yet generated enough statistics to analyse.

6. Results

In this section, we present preliminary results for the gradient flow β function of SU(2) with $N_f = 2$ flavours of adjoint Dirac fermion. The $N_f = 1$ theory, relying on the slower RHMC algorithm, has not produced sufficient data to reliably make an infinite volume extrapolation.

In all cases we generate data at the five volumes L^4, $L \in \{24, 28, 32, 36, 40\}$, with a molecular dynamics trajectory length $t_{len} \in [0.4, 2.0]$. In all cases we cut the first 2000 molecular dynamics time units (MDTU) for thermalisation, and we aim generate at least 6000 MDTU of thermalised data. However, some points in this contribution have fewer statistics than this, as ensembles were still being generated at the time of writing.

We extrapolate g_{GF}^2 and β in the $N_f = 2$ theory to the infinite volume limit using Eq. (1). Selected extrapolations are shown in Fig. 5. There remains some visible non-linear volume dependence at relatively large volume; this may be due to underestimated statistical uncertainties from low-statistics ensembles that currently lack sufficient ergodicity to give a good estimate of the statistical error.

In Fig. 6 we show how the range of running coupling and average plaquette spanned changes with N_{PV}. In contrast to previous work with smeared PV fields [3], where larger N_{PV} significantly
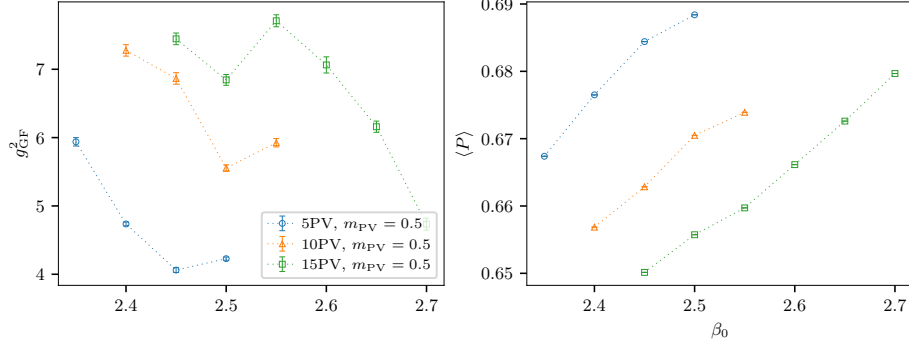
Figure 6: Plots of the running coupling and average plaquette as a function of the bare gauge coupling β_0, for $N_f = 2$, $N_{PV} \in \{5, 10, 15\}$, $m_{PV} = 0.5$. The three cases span a relatively similar range of g^2_{GF} and $\langle P \rangle$.
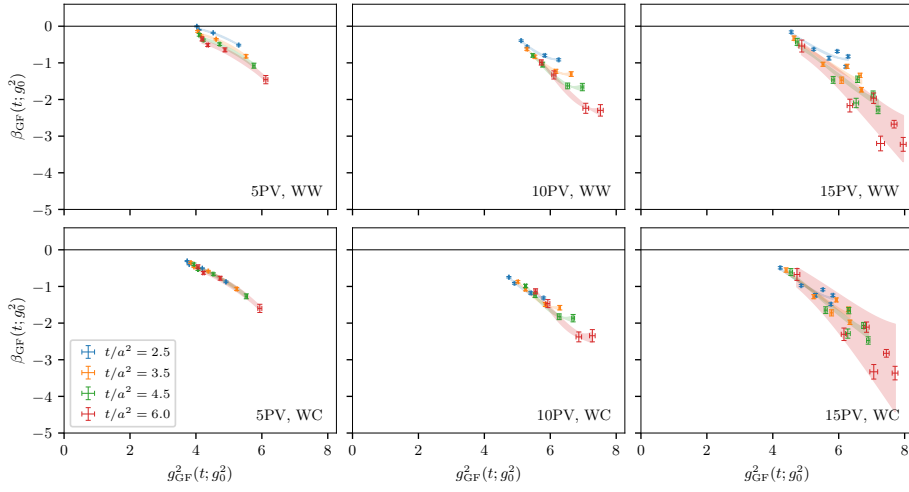

Figure 7: Plots of the gradient flow β function of SU(2) with $N_f = 2$ flavours of adjoint Dirac fermion, with $N_{PV} \in \{5, 10, 15\}$ PV fields (left to right), computed using the Wilson plaquette (upper) and symmetric clover (lower) operators.

raised $\langle P \rangle$, and allowed a larger range of g^2_{GF} to be spanned, in this case there is no significant shift in g^2_{GF} or $\langle P \rangle$, consistent with our expectations for unsmeared PV fields.

We may interpolate our data for β and g^2_{GF} using Eq. (2); this is a necessary step to eventually be able to take the continuum limit, to vary t at constant g^2_{GF}. We show these interpolations in Fig. 7. We observe that the data computed using the clover operator are significantly more consistent as t/a^2 increases (and hence the continuum is approached) than those computed with the plaquette operator; this matches our expectations that the clover operator should have fewer finite lattice spacing effects. The relatively narrow range of g^2_{GF} spanned, and the shift in g^2_{GF} as t/a^2 increases, means that the range of g^2_{GF} that could be interpolated at a wide range of t/a^2 is not sufficient to estimate the continuum β function for a useful range of g^2_{GF}.

7. Conclusions

We have computed the gradient flow beta function for SU(2) with $N_f = 2$ flavours of adjoint Dirac fermion, with the addition of $N_{PV} = 5$, 10, and 15 unsmeared PV fields. We have also studied

the parameter space of the equivalent $N_\text{f} = 1$ theory. Unlike results seen in work performed with smeared PV fields [4], we do not see a substantial change in the phase diagram or the range of running coupling that may be observed as N_PV is increased, instead only seeing a constant shift in the phase diagram as a function of the bare coupling; this is consistent with theoretical expectations.

We now aim to repeat this work with smeared PV fields, such that we may compute the β function at stronger coupling, including observing the fixed point in the $N_\text{f} = 2$ case, and any remnant of a fixed point in the $N_\text{f} = 1$ case.

Acknowledgements

Research Data Access Statement   The data generated for this manuscript can be downloaded from Ref. [15], and the workflow used to analyse it from Ref. [16]. The analysis workflow used to analyse the open data at Ref. [13] is available from Ref. [17].

References

[1] A. Athenodorou, E. Bennett, G. Bergner, P. Butti, J. Lenz and B. Lucini, *SU(2) gauge theory with one and two adjoint fermions towards the continuum limit*, 2408.00171.

[2] J. Rantaharju, *Gradient Flow Coupling in the SU(2) gauge theory with two adjoint fermions*, *Phys. Rev. D* **93** (2016) 094516 [1512.02793].

[3] A. Hasenfratz, Y. Shamir and B. Svetitsky, *Taming lattice artifacts with Pauli-Villars fields*, *Phys. Rev. D* **104** (2021) 074509 [2109.02790].

[4] A. Hasenfratz and C.T. Peterson, *Infrared fixed point in the massless twelve-flavor SU(3) gauge-fermion system*, *Phys. Rev. D* **109** (2024) 114507 [2402.18038].

[5] L. Del Debbio, A. Patella and C. Pica, *Higher representations on the lattice: Numerical simulations. SU(2) with adjoint fermions*, *Phys. Rev. D* **81** (2010) 094503 [0805.2058].

[6] C. Pica and HiRep contributors, *HiRep* (2024). github.com/claudiopica/HiRep.

[7] S. Martins, E. Kjellgren, E. Molinaro, C. Pica and A. Rago, *GPU-accelerated Higher Representations of Wilson Fermions with HiRep*, *PoS* **EuroPLEx2023** (2024) 035 [2405.19294].

[8] O. Tange, *GNU Parallel* (2023). doi:10.5281/zenodo.11043435.

[9] L. Del Debbio, B. Lucini, A. Patella and C. Pica, *Quenched mesonic spectrum at large N*, *JHEP* **03** (2008) 062 [0712.3036].

[10] M. Lüscher, *Properties and uses of the Wilson flow in lattice QCD*, *JHEP* **08** (2010) 071 [1006.4518].

[11] F. Mölder et al., *Sustainable data analysis with snakemake*, *F1000Research* **10** (2021) .

[12] F. Joswig et al., *pyerrors: A python framework for error analysis of Monte Carlo data*, *Comput. Phys. Commun.* **288** (2023) 108750 [2209.14371].

[13] A. Hasenfratz and C. Peterson, *Twelve flavor SU(3) gradient flow data for the continuous beta-function* (2024). doi:10.5281/zenodo.10719051.

[14] E. Bennett, A. Athenodorou, G. Bergner, P. Butti and B. Lucini, *Towards the β function of SU(2) with adjoint matter using Pauli–Villars fields* (2024). doi:10.5281/zenodo.13361520.

[15] A. Athenodorou, E. Bennett, G. Bergner and B. Lucini, *Towards the β function of* SU(2) *with adjoint matter using Pauli–Villars fields—data release* (2024). doi:10.5281/zenodo.13128505.

[16] A. Athenodorou, E. Bennett, G. Bergner and B. Lucini, *Towards the β function of* SU(2) *with adjoint matter using Pauli–Villars fields—analysis workflow* (2024). doi:10.5281/zenodo.13128384.

[17] E. Bennett, *Alternative analysis workflow for "Twelve flavor SU(3) gradient flow data for the continuous beta-function"* (2024). doi:10.5281/zenodo.13362605.